U.S. DEPARTMENT OF THE INTERIOR

U.S. GEOLOGICAL SURVEY

LOW STRAIN LEVEL ACOUSTIC EMISSION DUE TO SEISMIC WAVES AND TIDAL/THERMOELASTIC STRAINS OBSERVED AT THE SAN FRANCISCO PRESIDIO, CALIFORNIA

Baxter H. Armstrong[1]
IBM Scientific Center
1530 Page Mill Road
Palo Alto California 94306

Carlos M. Valdes-Gonzales
Department of Geology and Geophysics
Univeristy of Wisconsin, Madison, Wisconsin 53706

Malcolm J.S. Johnston
U.S. Geological Survey
Menlo Park, California 94025

James D. Leaird
Physical Acoustics Corp.
Roseville, California 94661

Open-File Report 93–583

1993

[1]Now at U.S. Geological Survey, Menlo Park, CA

TABLE OF CONTENTS

ABSTRACT

Acoustic Emission (AE) event recordings were made with 30 and 110 kHz resonant piezoelectric transducers and a 1 Hz to 20 kHz accelerometer at the San Francisco Presidio during the times of the Lake Elsman earthquake and its largest aftershock on August 8, 1989, the Loma Prieta earthquake aftershocks of October 17, 1989, and a small earthquake on the Hayward fault in November 4, 1989. Each earthquake generated abrupt increases in AE production at the time of arrival of the seismic waves that were clearly above the background rates. Corresponding strain changes recorded on strainmeters in the same thermally insulated test bunker are from a few tens to a few hundreds of nanostrain, with strain rates from $\approx 5\times10^{-7}s^{-1}$ to $\approx 10^{-5}s^{-1}$. Sensitivity of AE to tidal strains was checked by comparison of the 30 kHz background AE and the strain recorded by one of the USGS strainmeters during a 30-day interval in April and May, 1991. At this site tidal strains are greater than thermoelastic strains at semi-diurnal periods. Power spectral densities and coherence were computed for the strain and AE data. Dominant spectral peaks at approximately 24 hours (O_1, k_1, S_1, M_1, etc., tidal periods) and approximately 12 hours (O_2, k_2, S_2, M_2 etc., tidal periods) are clear in the strain spectrum and suggested in the AE spectrum. A weak correlation between the rate of AE production and the observed strain is observed at these near-diurnal and semidiurnal periods. This suggests that AE production occurs at strain levels and strain rates even lower than those estimated to be caused by passage of seismic waves from the 1989 earthquakes. We believe these to be the lowest strain levels and strain rates for which acoustic emission has been reported.

1. INTRODUCTION

The term Acoustic Emission (AE) refers to elastic-wave pulses with frequencies in the range from a few kHz to a few MHz generated within solids subjected to stress loading. Sources of these pulses include opening and closing of cracks, pore collapse, grain boundary sliding and dislocation motion. Detailed description of methods for the detection, measurement and characterization of AE during the last 30 years can be found in Lord (1975), Lord (1981), Momoh, *et al.* (1989), and Vladut and Lepper (1989). The traditional use of AE has been in non-destructive testing and study of rock failure (e. g., Lockner, *et al.*, 1991), and has been limited to relatively high strain levels, typically above 10^{-5}.

AE in the range of 1 kHz to 150 kHz is highly attenuated in the earth, with propagation distances of no more than a few hundreds of meters for 1 kHz waves, and a few tens of meters for 150 kHz waves. These distances are short compared to the distances traveled by seismic waves. It was suggested that AE may be generated during the strain buildup prior to earthquakes (termed "secondary AE") (Armstrong, 1983). Secondary AE in the range of 20 to 30 Hz is also triggered by seismic waves at substantial distances from the source (Armstrong and Stierman, 1989). Such secondary AE is produced at strain amplitudes and strain rates much lower than those for which AE has generally been studied and observed before.

Few observations or experiments have been made of AE at low-strain amplitudes expected to occur in an earthquake-preparation zone. AE triggered in the Lehman Cave National Monument in Nevada by a small earthquake 12 miles away was

reported by Repsher and Steblay (1985). Hardy and Ersavci (1988) have reported secondary AE in a mine environment; this is further discussed by Hardy, Belesky, and Mrugala (1988), who introduce the concept of a "conversion zone" containing material subject to processes or conditions (e. g., residual stress) that permit the generation of AE by the strain field from a remote source. It seems fair to say, however, that until now there has not been an adequately confirmed identification of secondary AE. Some laboratory observations of AE at strain levels between 10^{-4} and 10^{-6} and over a range of rates down to about 10^{-9} s^{-1} are reviewed by Armstrong and Valdes (1991).

The objective of the present work was to determine:

[1] whether AE in the range of a few kHz to about 100 kHz is generated by the arrival of seismic waves from local or teleseismic earthquakes and

[2] whether AE is generated by earth tides at strain levels below 10^{-7} and at strain rates below 10^{-12} s^{-1}.

AE arising from tidal variations could demonstrate the existence of AE at levels of interest in earthquake-preparation zones. Our study is analogous to those of Diakonov, *et al.* (1990) and Galperin, *et al.* (1990). These authors studied the possibility of "seismic emission" of seismic waves due to solid-earth tidal strain and teleseismic waves with strains of the order of 10^{-8} in a range upward from about 30 Hz to a few hundred Hz.

Little energy is required to generate AE signals at 30 kHz. If we assume that a volume several wavelengths on a side is required to produce a well-defined wave, this volume is about 0.5 m^3 or less for 30 kHz but is about 10^9 m^3 for a 30 Hz wave. Thus, for 30 kHz AE excitation, we are dealing with microscopic source sizes, as opposed to the macroscopic source sizes required to produce seismic waves of kilometer wavelengths.

In principle, AE events with stress amplitudes down to at least 10^{-2} microbars can be detected (Lord, 1982). For a material such as concrete or sandstone, the bulk modulus is about 10^{11} dyne cm^{-2}. A stress amplitude of 10^{-2} dyne cm^{-2} implies a strain of the order of 10^{-13} in such a material. This, as one would expect, is somewhat lower than strains that are resolved by instruments in the traditional seismic regime where localized near-surface strains of 10^{-9} are common. (Strains of 10^{-11} are about the current limit of resolution; see Borcherdt, *et al.*, 1989). It should not be surprising, therefore, for a strain excitation of the order of 10^{-8} to 10^{-9} to trigger low-level strain events in the 10^{-12} to 10^{-13} range.

2. EXPERIMENTAL SITE AND INSTRUMENTATION

The US Geological Survey (USGS) instrument vault at the San Francisco Presidio (lat. 37.79, long. 122.47) was originally constructed as an ammunition bunker during the Spanish-American war. It houses strainmeters, tiltmeters, seismometers and a variety of other geophysical instruments (Jones, 1983). It is built on Franciscan chert and sandstone on top of a hill, overlooking the Pacific Ocean near the Golden Gate bridge, approximately 10 km east of the San Andreas fault. The walls are reinforced concrete approximately 1/2 meter thick, and the roof is heavily reinforced with steel girders. The interior rooms can be isolated from one another. Few sandstone outcrops

are found in the area, although two cores through the floor of the bunker show weathered sandstone directly below. The bunker is covered by earth fill which reaches approximately 7.5 m at the center and 3.5 m at the edges of the bunker. This overburden provides substantial thermal insulation such that the temperature changes less than 0.05°C per day and 0.5°C per year. Earth strain tides recorded at this site have amplitudes of about 10^{-7} where about half of this results from loading from the nearby Pacific Ocean. The strain tides are greater in amplitude than diurnal thermoelastic strains, both in the ground and in the building, and the site therefore provides an ideal location for comparing a known strain signal with the output from AE detectors. Fig. 1 shows the configuration of the Presidio observatory and the location therein of our instruments.

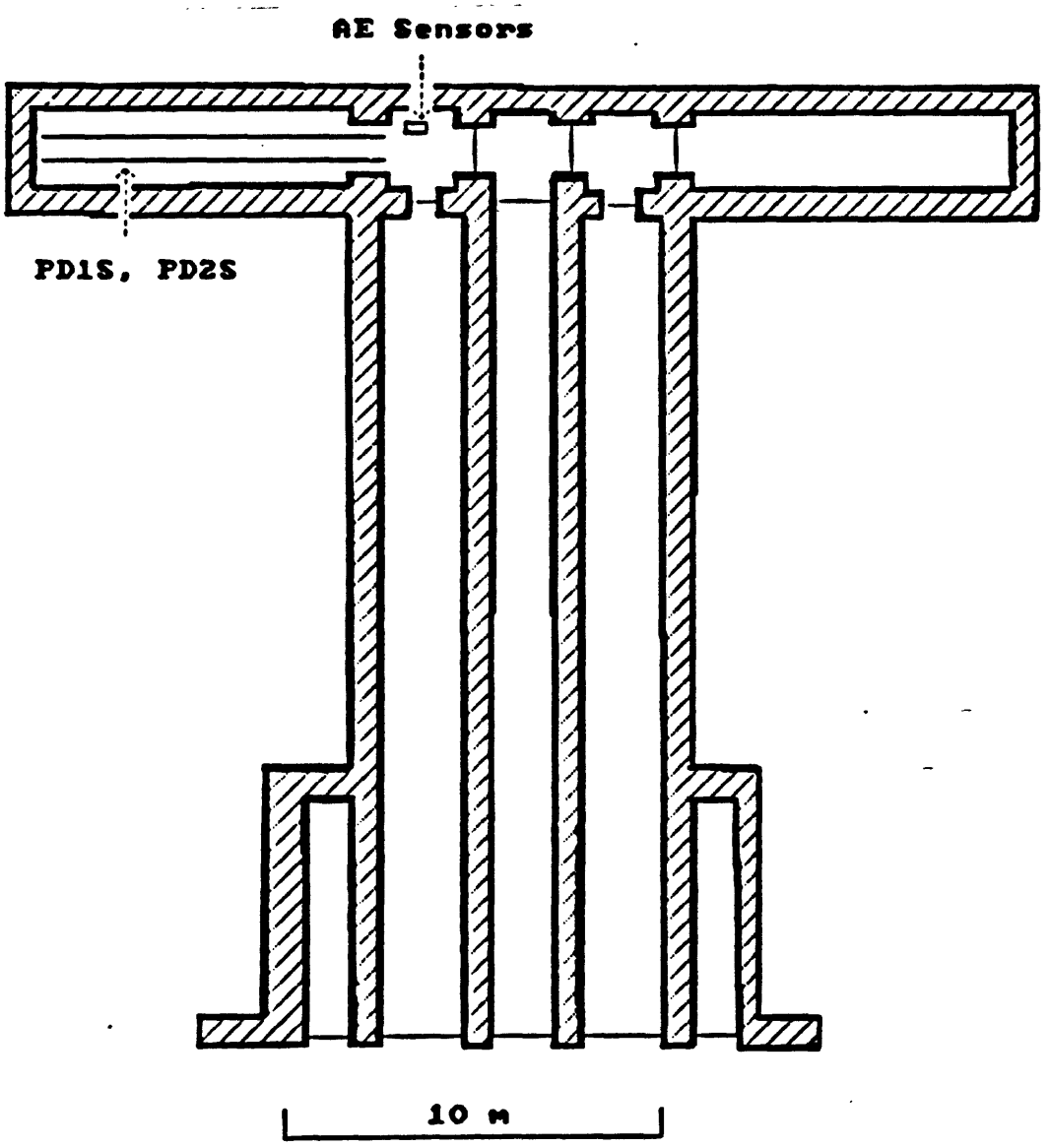

Fig. 1. Plan view of the Presidio Observatory. This site houses a seismometer, strainmeters, tiltmeters, and a precision thermometer operated by the USGS. Our AE sensors were installed in the same room where the PD1S and PD2S strainmeters are located as shown in the figure.

Data from the USGS strainmeters and tiltmeters are sampled every ten minutes and transmitted to the USGS offices in Menlo Park. Because of this low sampling rate, transient disturbances with durations shorter than ten minutes (such as for seismic waves) are not detected in the telemetered data but are recorded on site. The USGS instruments are located 40 m from the entrance to the bunker and are separated from the entrance by a system of four doors that provides a 16 ± 0.01°C temperature-stable room. Narrow-gauge (about 0.5 m apart) iron rails are embedded in the concrete floor of some of the rooms. One end of each of the strainmeters PD1S and PD2S was anchored to each of a pair of these rails.

In June, 1989, we installed two AE sensors in the same room where the PD1S and PD2S strainmeters are located (Fig. 1). These piezoelectric sensors, type AET AC 100, and AET 8-A1.03, have resonant frequencies of 110 and 30 kHz, respectively. They are part of the usual acoustic emission system consisting of sensor, preamplifier, and filter. The 30-kHz sensor signal is passed through a 15 - 45 kHz bandpass filter and the signal from the 110 kHz sensor is subjected to a 1 kHz - 100 kHz filter. On September 26, 1989, the 110 kHz sensor was replaced by a 1 Hz-20 kHz sensor (B & K model 4375). This model 4375 sensor was placed in line with the same 1 kHz - 100 kHz bandpass filter. The 4375 sensor had a lower apparent noise rate (about 6 events/hour) and considerably less sensitivity than the 30 kHz sensor.

Initially these sensors were taped snugly against well-cleaned spots on the concrete bunker floor about .5 m apart and about .5 m from one end of strainmeter PD1S. Over time, we progressively improved the coupling of the sensors to the concrete floor by adding grease as a couplant and covering the sensors with sand. Eventually (Nov. 11, 1989 and thereafter), beeswax was used to improve coupling. On December 27, 1989, the B & K Model 4375 sensor was removed and the 30 kHz sensor was relocated to a point down the rail about 2 m from the end of strainmeter PD1S. (The strainmeter PD2S was anchored symmetrically to PD1S on the other rail of the pair.) Thus, the position of our 30 kHz sensor was roughly 2 m from one end of both strainmeters after Dec. 27. This proved to be a good location from the standpoint of noise and instrument sensitivity. A sand cover was added to protect the sensors from airborne noise and insects.

The 30 kHz sensor is in a stainless steel canister 7.75 cm in height, 3.5 cm in external diameter and 2.9 cm in internal diameter. The piezoelectric crystal is secured within and against the bottom of the cylinder with an epoxy-type cement. There is a 1.5 cm high air space above the crystal within the canister. The sensor is connected (by cable) to the input of the preamplifier through a decoupling capacitor.

Signal processing, storage and display were performed with the Acoustic Emission Technology Corp. Model 204B acoustic emission monitoring system designed to detect and process the emissions from microseismic activity and other sources of acoustic emission. Our operations were generally conducted with a total amplification of 98 dB, including the preamplification (40 dB) and the amplification within the 204B system. The output from the system, viz. number of events vs time, was plotted using a strip-chart recorder with a speed of 2 hr/cm and a timing accuracy of about 4 minutes. The AE data monitoring system counts the number of AE events that exceed a preset threshold level, chosen to be above the electronic and AE noise level. Because the "AE noise level" is not well defined; we measure all events above system

and electronic noise. The output was viewed on an oscilloscope periodically to check the integrity of the system. All AE events used in the analyses given below were counted during periods of stable operation.

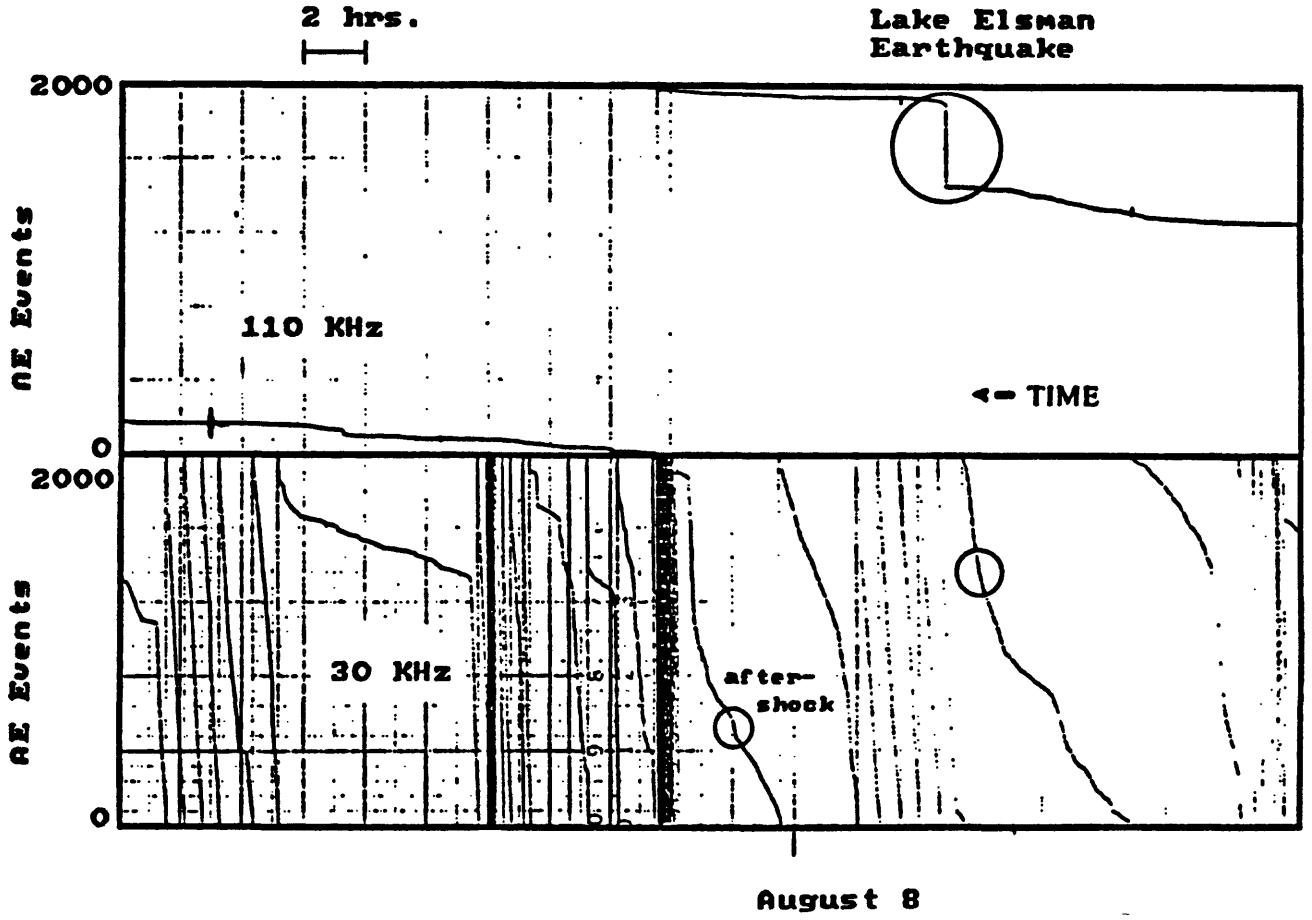

Fig. 2. Cumulative plot of the number of AE events against time for the 30 kHz (bottom) and 110 kHz (top) sensors during the August 8, 1989, Lake Elsman earthquake.. Increasing time runs from right to left, and the pen resets to 0 when it accumulates 2000 events. The top trace is offset ahead by one hour from the bottom trace. A circle encloses the increase in rate of events on the 30 kHz trace at the time of the earthquake. An increase of 470 events on the 110 kHz trace at the time of the M_L 4.5 Lake Elsman aftershock is also marked with a circle.

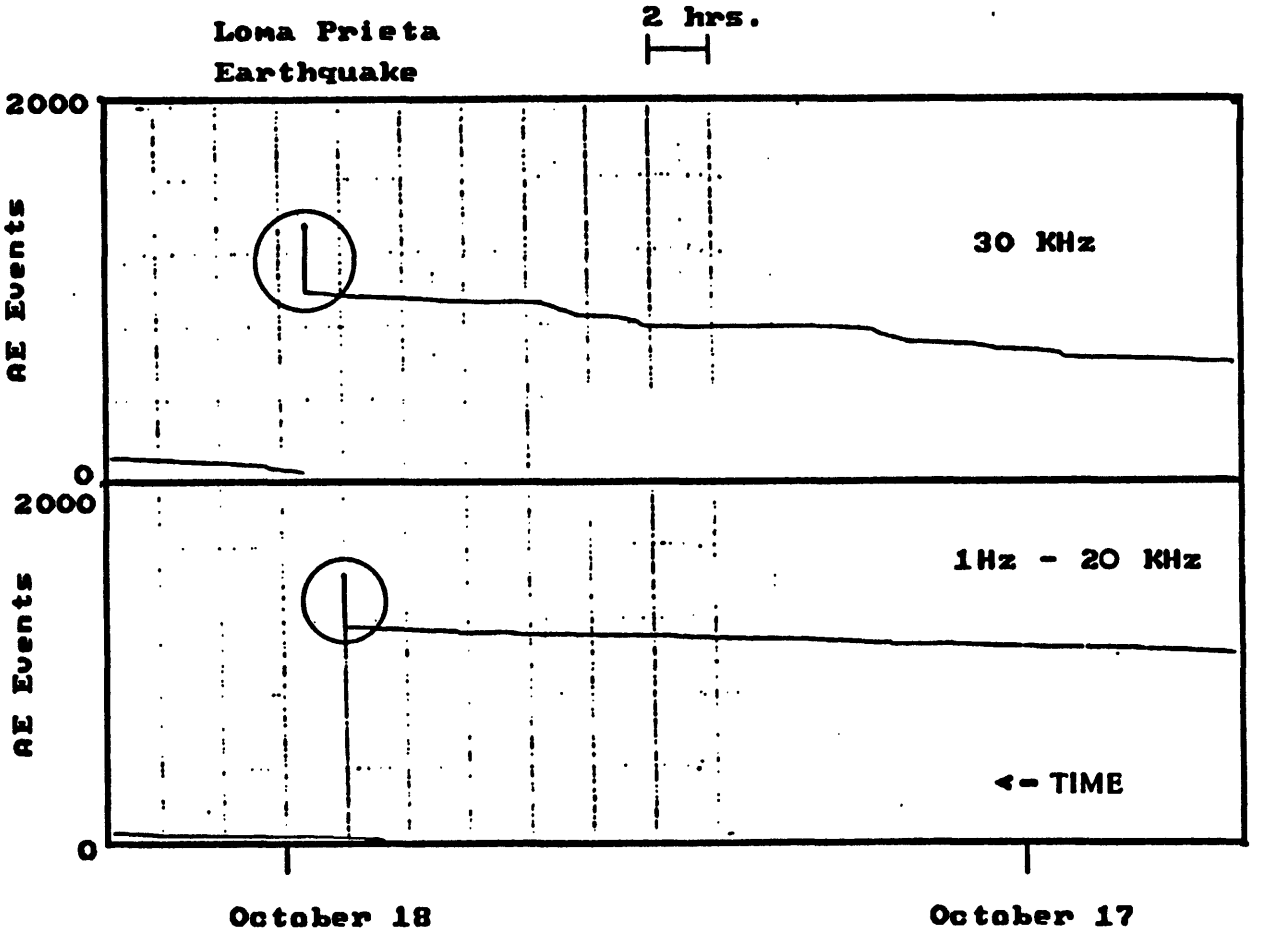

Fig. 3. Cumulative plot of number of AE events for the 1 Hz - 20 kHz (bottom) and 30 kHz (top) sensors immediately before the October 18, 1989, M_L 7.1 Loma Prieta earthquake. Increasing time runs from right to left as in Fig. 2, and the top trace is one hour ahead of the bottom trace.. Circles mark the time of the earthquake when the power failed and remained off for 3 days.

3. 1989 LAKE ELSMAN AND LOMA PRIETA EARTHQUAKE OBSERVATIONS

The M_L = 5.1 Lake Elsman earthquake of August 8, 1989, at 08:13 UTC occurred on the San Andreas fault 85 km south of our San Francisco Presidio location and about 15 km from the hypocenter of the Loma Prieta quake that occurred a few months later. Our 110 kHz sensor registered a 470-event step increase at the time of the Lake Elsman earthquake (within the four-minute time resolution of our strip-chart recorder) upon a fairly regular background rate of about 19 events/hr average for the three hours preceding the earthquake, and ≈ 8 events/hr afterward (Valdes and Armstrong, 1989). Fig. 2 shows this record as the upper part of the figure. It is a cumulative plot of the number of AE events against time. As in all the strip-chart figures, time runs from right to left, and the pen resets to 0 when it accumulates 2000 events. The top trace is offset to be one hour ahead of the bottom trace in order to avoid conflict between the marking pens.

The 30 kHz sensor was experiencing a high background rate, emphasized by the continual resetting of the recording pen because of a low threshold setting, as can be seen in the lower portion of Fig. 2. However, a marginally recognizable increase in slope of events *vs* time from the 30 kHz sensor at the time of the earthquake is enclosed by a circle. A small increase of 40 events from the 30 kHz sensor occurred at the time (August 8, 1989 at 15:44 UTC) of the M_L = 4.0 Lake Elsman aftershock, and is also enclosed by a circle on the figure. The 110 kHz sensor did not respond perceptibly to this aftershock. These signals on the 30 Khz sensor seem well within the noise levels.

The Loma Prieta M_L = 7.1 earthquake of October 17, 1989 (17:04 local time) occurred, as noted above, about 15 km from the Lake Elsman earthquake. We obtained no useful data during and for 7 days following this event because of the electrical power outage that accompanied the earthquake. The noise background prior to the Loma Prieta quake as seen in Fig. 3 is marked by a number of small, but distinct steps or unknown origin. Fig. 3 again is a cumulative plot of number of AE events against time running backward as in Fig. 2. On October 25, after our instruments were back in operation, there was a series of many aftershocks, including one of magnitude 4.4 and one of magnitude 3.8. These are marked, along with numerous smaller aftershocks, on the AE response record of Oct. 25 and 26 shown in Fig. 4. The AE event rate for the 30 kHz sensor is variable and at times quite high over this time period, which was a time of high seismic aftershock activity (approximately one aftershock per hour with M_L greater than 2.0). Over the 6-hour periods preceding and following the 4.4 October 25 aftershock, the 30 kHz sensor was registering a background rate exceeding 100 events/hr. No change, however, is observed in the 1 Hz-20 kHz sensor. Many abrupt steps appear in the 30 kHz AE event rate for the period following the Loma Prieta earthquake that are not coincident with an aftershock but are clearly separated from the normal background. However, the rate at which this AE activity occurs decreases with time as the Loma Prieta aftershock activity dies out. The total background AE level, continuous plus the steps mentioned above, appeared higher during the aftershock period of the Loma Prieta quake than before the quake, and by February, 1990 and thereafter we observed a generally uniform background marked by only occasional small steps.

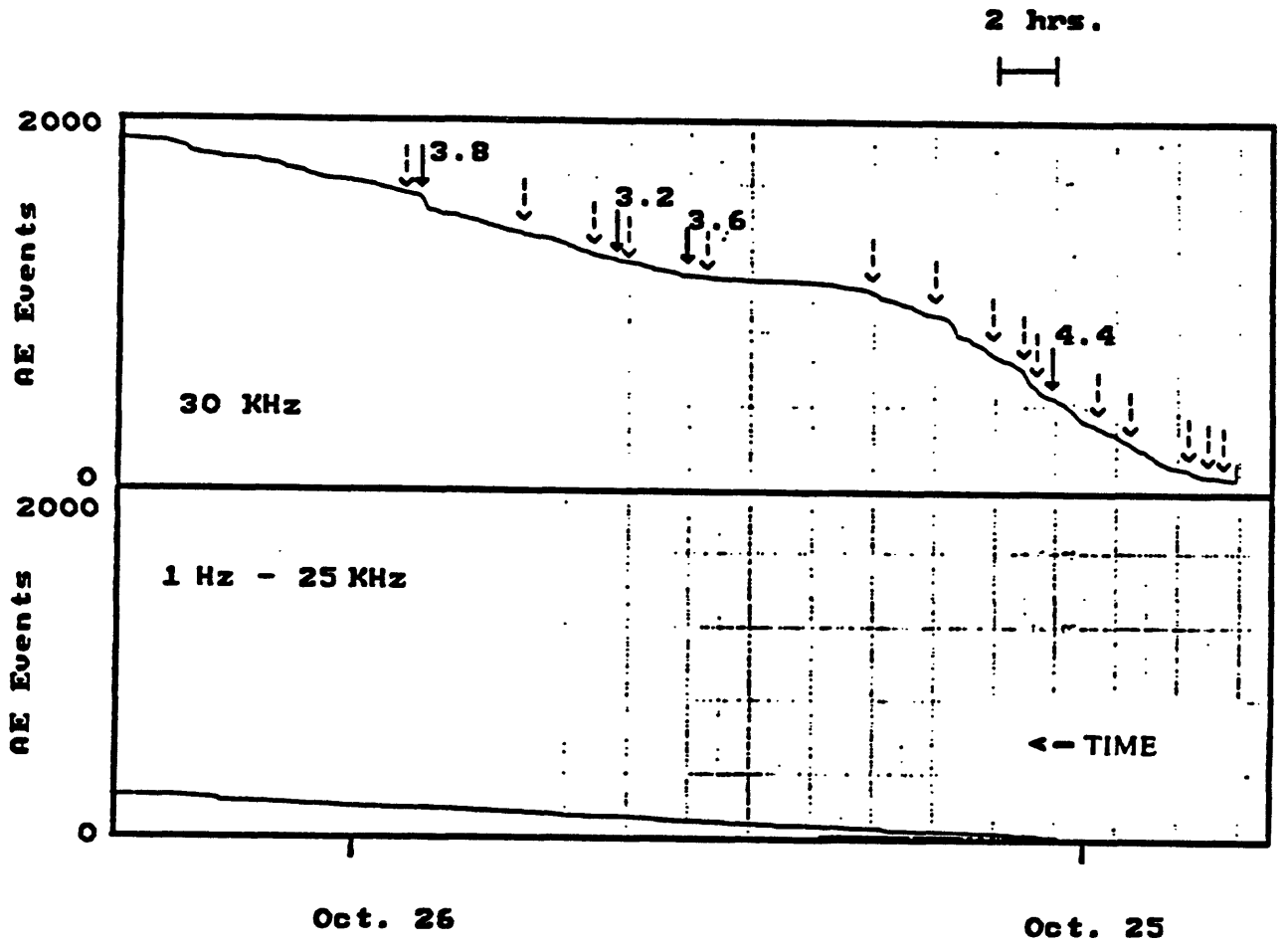

Fig. 4. Cumulative number of events from the 1 Hz - 20 kHz (bottom) and 30 kHz (top) sensors from about 18:00 UTC, October 24, 1989, to about 08:00 October 26, 1989, during aftershocks of the Loma Prieta earthquake. The largest being a M_L 4.4 on October 25 that was preceded by five events with M_L greater than 2. This period of high seismicity coincided with high 30 kHz AE activity, as shown in the figure. Note that time again runs from right to left, and that the top trace is one hour ahead of the bottom trace.

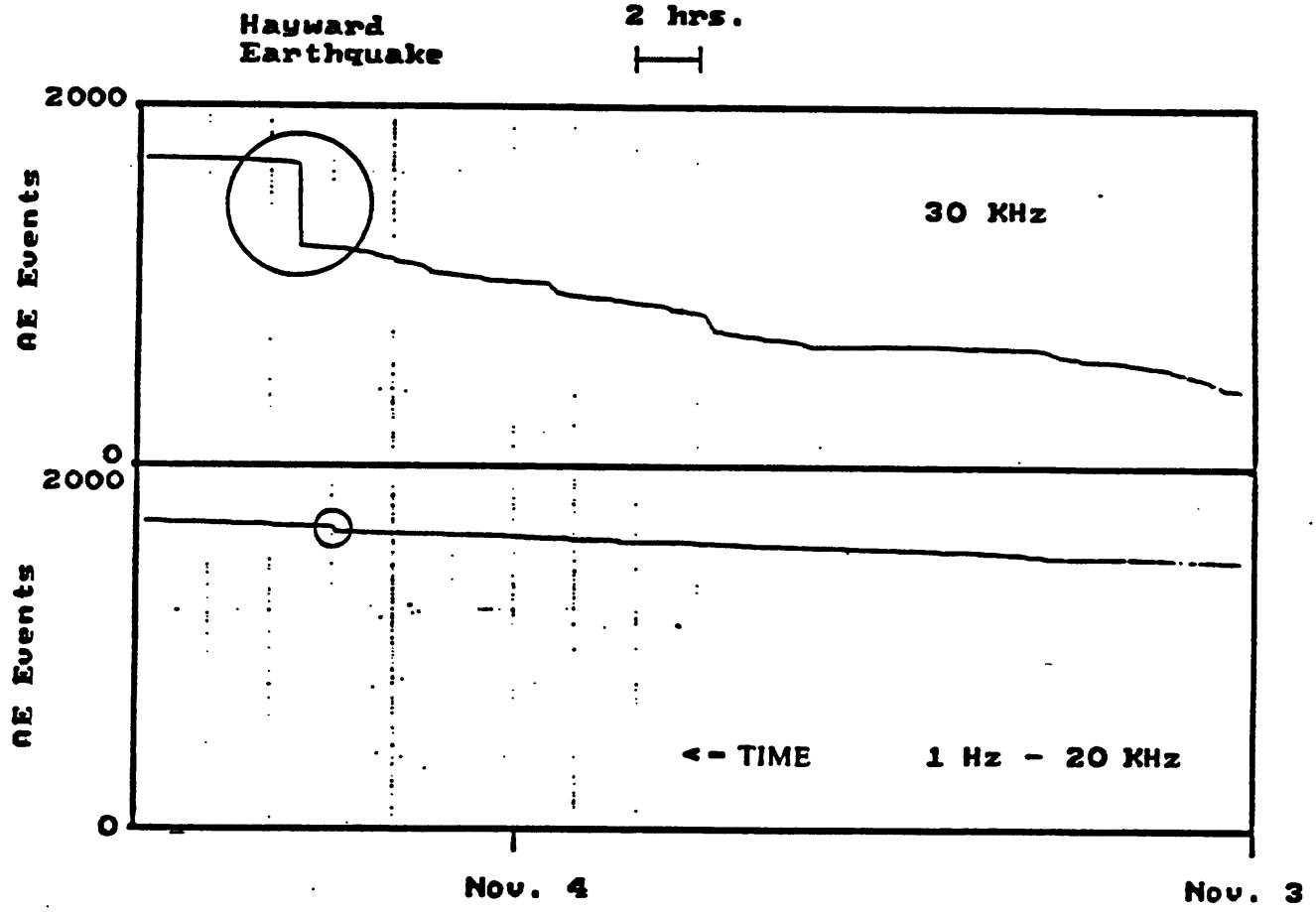

Fig. 5. Cumulative number of AE events from the 1 Hz - 20 kHz (bottom) and 30 kHz (top) sensors from November 3, 1989, to 12:00 UTC, November 4, 1989, during the time of the November 4, 1989, M_L 3.7 earthquake at 07:16 UTC on the Hayward fault. The 420 event jump on the 30 kHz record occurs at the time of the earthquake. The 1 Hz - 20 kHz sensor shows a 30 event increase at the time of the earthquake. Note that time runs from right to left, and the top trace is one hour ahead of the bottom trace.

On November 4, 1989, at 07:16 UTC there was a M_L= 3.7 event on the Hayward fault with epicenter located 25 km from the Presidio. Fig. 5 shows AE jumps of 35 and 420 events for the B & K 4375 and 30 kHz sensors, respectively, at the time of this earthquake, within our 4-minute time resolution window. The slope of this cumulative plot shows that the 30 kHz sensor was experiencing an average rate of about 30 events/hr over the four hours before the quake. This rate dropped to about 5 events/hr afterward. The 4375 sensor showed a uniform background noise rate of about 7 events per hour before and after the earthquake. In both cases, the jumps are clear and unambiguous upon the background.

4. EARTHQUAKE STRAIN AND STRAIN RATE ESTIMATES

Ground-displacement amplitudes were calculated using the magnitudes M_L, for each of the earthquakes in the relation given by Richter (1958) and neglecting resonance effects within the Presidio vault. A sine wave with this amplitude and with a frequency corresponding to the dominant frequency of the wave train was differentiated with respect to displacement and time to obtain the strain and strain rate, respectively. For each of the Lake Elsman earthquake, its aftershock, and the Hayward fault earthquake, this dominant frequency was taken to be 2 Hz while the seismic wave velocity was taken as 3 km/s. Table I shows the results of these order-of-magnitude estimates. From this table, we see that the strain level of the seismic wave from the Lake Elsman aftershock is of the same order of magnitude when it reaches the Presidio as that associated with earth tides, although the strain rate is considerably higher.

TABLE I - Estimated strain amplitude increments (top row), and strain rates (bottom row in s^{-1}) for seismic radiation from the August 8, 1989 Lake Elsman earthquake and aftershock, and the Nov. 4, 1989, Hayward fault earthquake.

Source	Lake Elsman, 85 km M=5.1 Earthquake	Lake Elsman, 85 km M=4.3 Aftershock	Hayward Flt, 25 km M=3.7 Earthquake
$\Delta\varepsilon$	$\approx 2\times10^{-7}$	$\approx 4\times10^{-8}$	$\approx 10^{-7}$
$\dot{\varepsilon}$	$\approx 3\times10^{-6}$	$\approx 5\times10^{-7}$	3×10^{-6}

5. STRAIN AND ACOUSTIC EMISSION

An important objective of this work was to test whether AE is generated as a result of tidal strains. The primary advantage in selecting the USGS Presidio vault for the experiment is that more then 10 years of strain and temperature data have been collected and these measurements are well understood. Thermoelastic strains, whether in the ground or in the structure, are smaller in amplitude than tidal strains. An interval of approximately 30 days in April and May of 1991 was selected for comparison of the 30 kHz background AE with the strain recorded by one of the USGS

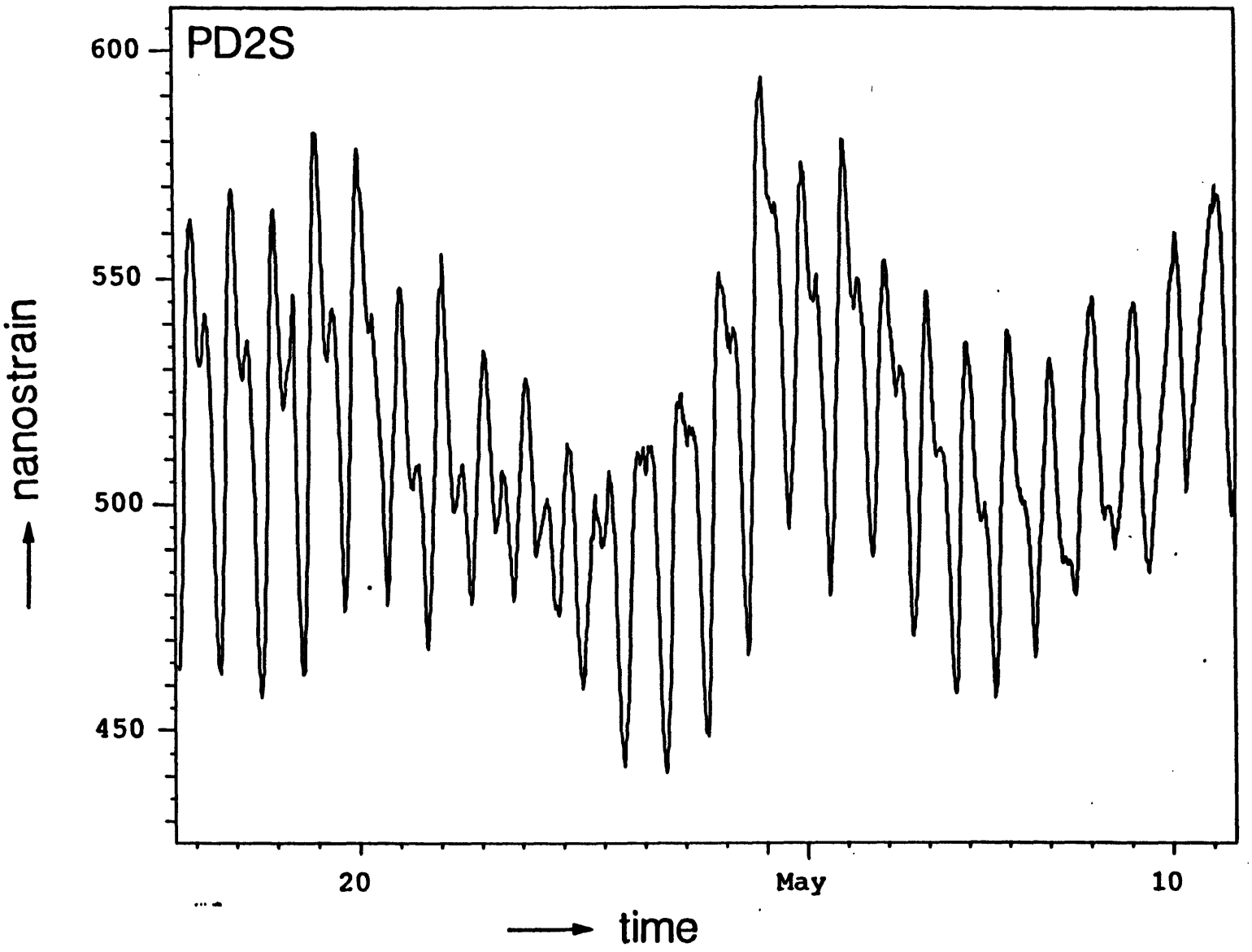

Fig. 6. Detrended strain record in nanostrain from instrument PD2S in the Presidio vault observed from April 15, 1991 to May 11, 1991. The sampling rate is one sample per 10 minutes.

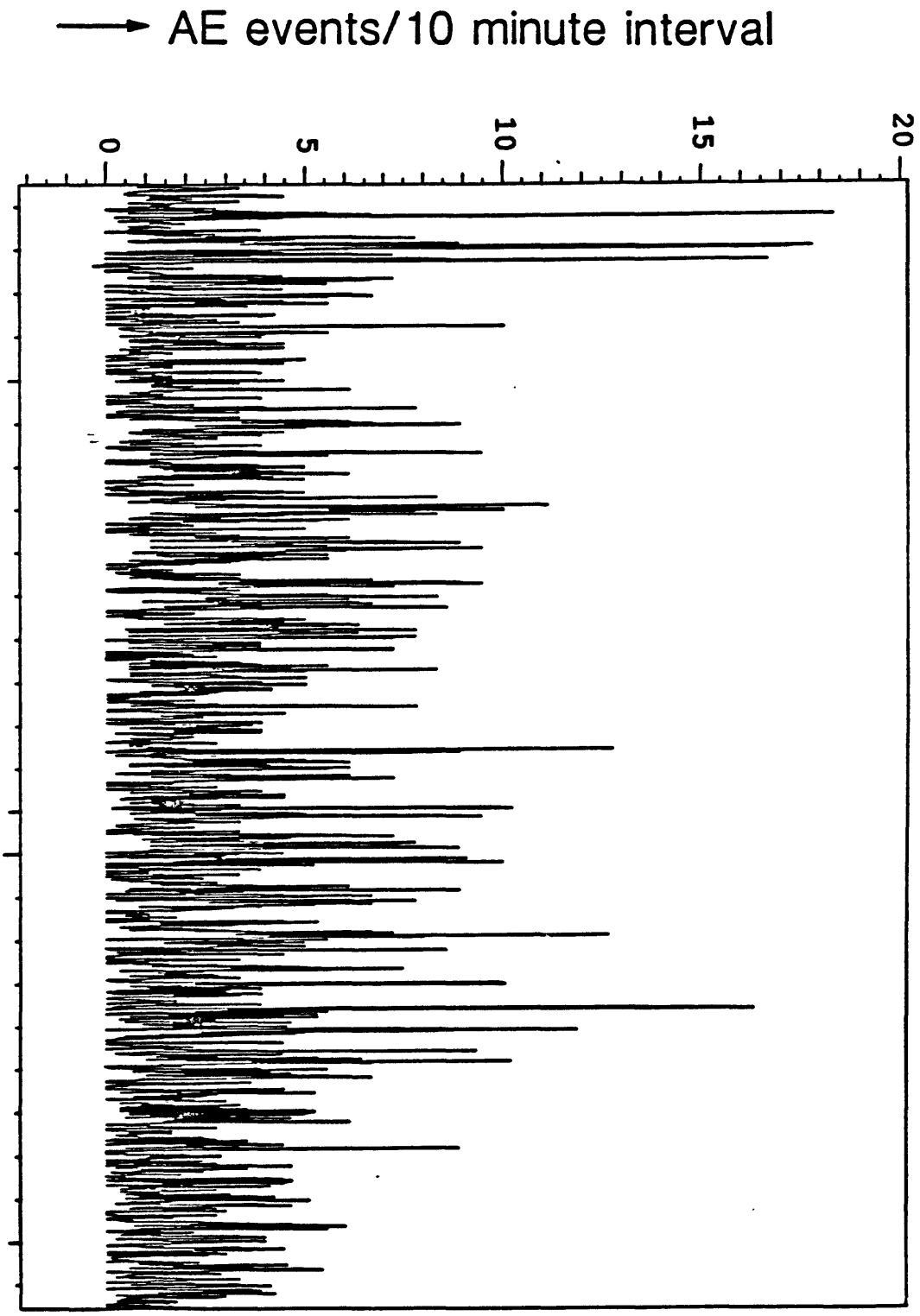

Fig. 7. The number of 30 kHz acoustic emission events per 10-minute interval observed in the Presidio vault from April 15, 1991 to May 11, 1991.

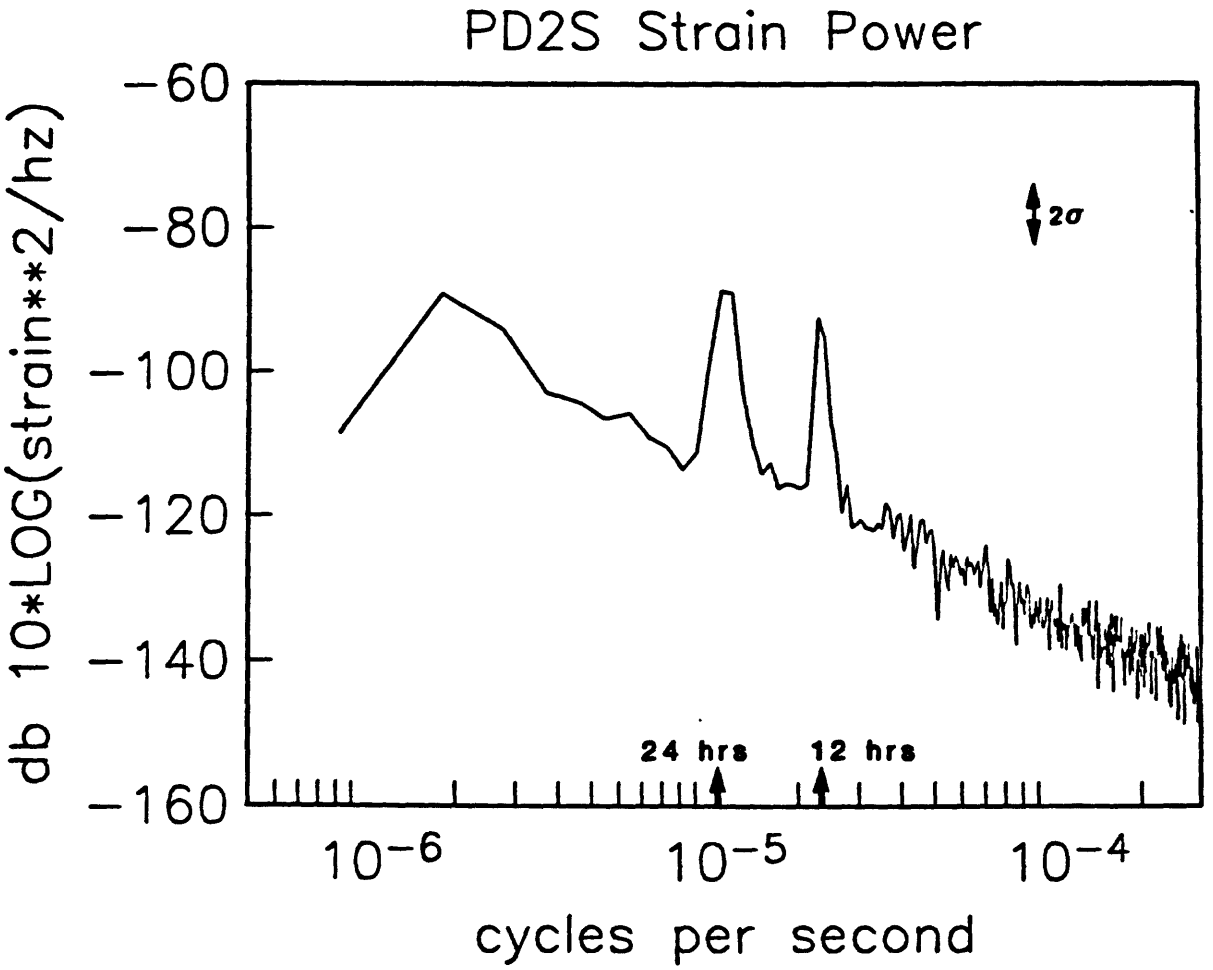

Fig. 8. Power spectral density of the strain record of Fig. 6. The spectral amplitude is in dB relative to a power level of 1 ε^2 Hz^{-1}. The upward arrows mark periods of 24 and 12 hours.

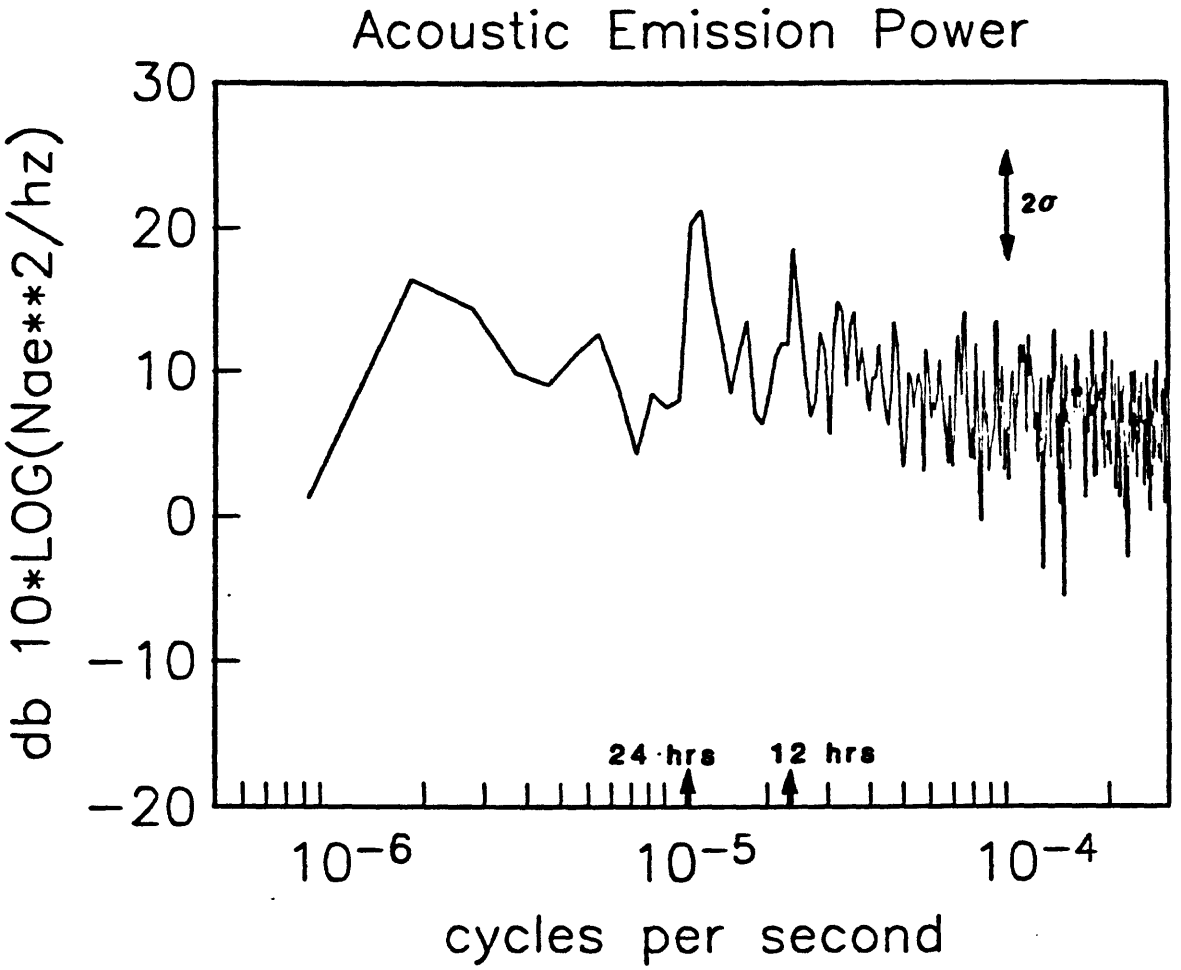

Fig. 9. Power spectral density of the acoustic emission data of Fig. 7. The spectral amplitude is in dB relative to 1 count^2 Hz^{-1}. The upward arrows mark periods of 24 and 12 hours.

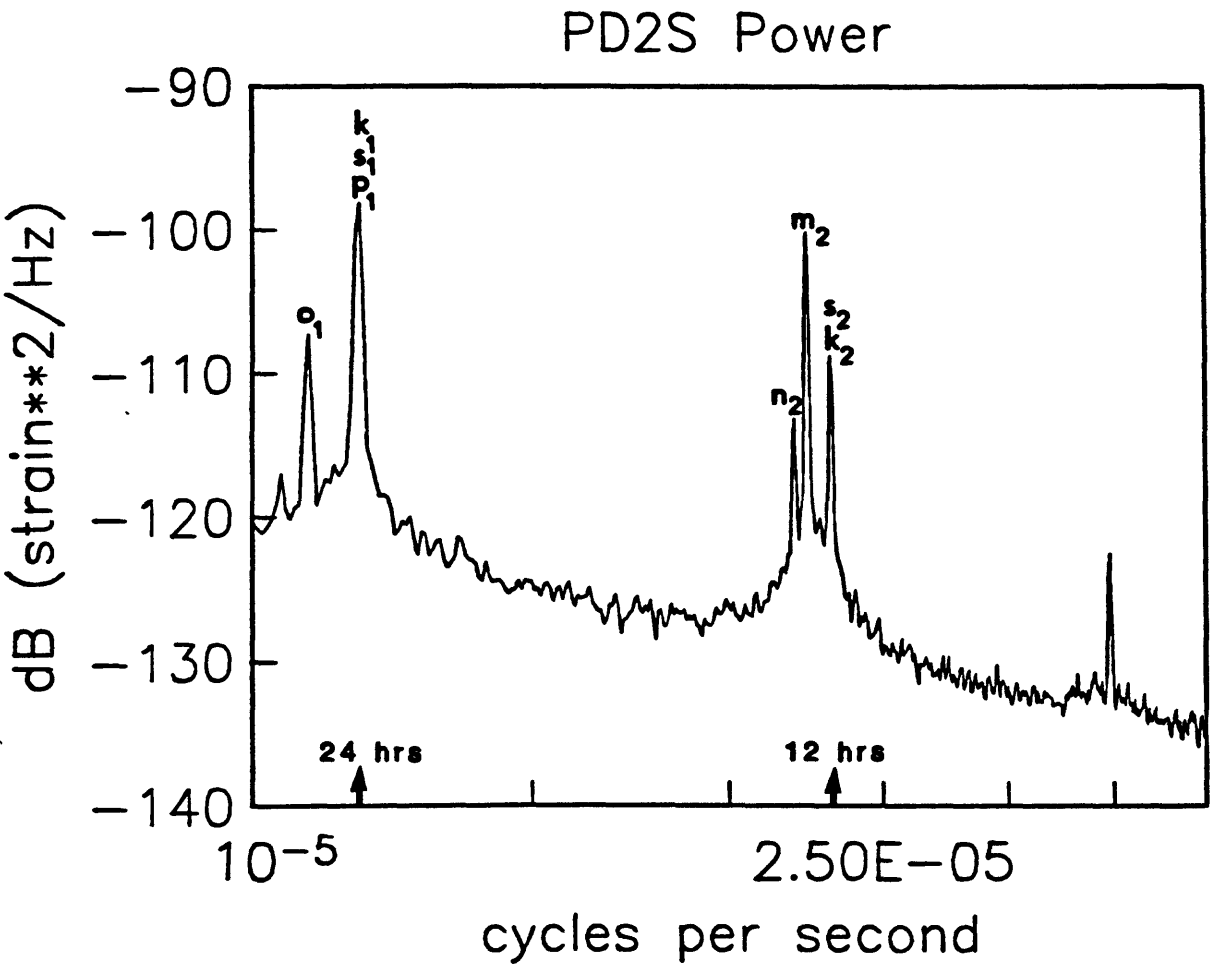

Fig. 10. Power spectral density of an extended (3 year) strain record at the Presidio vault chosen to illustrate some of the diurnal and semidiurnal tidal components.

strainmeters. Power spectral densities and coherence were computed for the strain and AE data. Fig. 6 shows the detrended 10-minute sample rate strain record in nanostrain for instrument PD2S for the time interval 04:15 April 15, 1991 to 12:30 May 11, 1991 (UTC). Primary features of the record are diurnal and semidiurnal signals due mainly to earthtides and some longer term variations with duration of about a week. The peak-to-peak strain levels each day are of the order of 100 ns. This corresponds to incremental strain of less than 1 nanostrain per 10-minute sampling interval. Fig. 7 shows the 30 kHz AE data over the same span of time. In order to match the timing of the strain data, these data were manually digitized from the paper chart at 10-minute intervals. The number of AE events per 10-minute interval is plotted on the abcissa with the mean rate of AE production being 2.3 events per 10-minute interval.

To make a more quantitative comparison between the strain and the AE data, we examined the power spectra of each. This analysis is limited because of the short length of data (4143 values). Nevertheless, this short sample is adequate to allow preliminary estimates of spectral amplitude and coherence to be made. Fig. 8 shows the power spectrum as a function of frequency obtained from the strainmeter data. Spectral amplitudes are in dB referenced to a power level of 1 $\varepsilon^2 Hz^{-1}$. Fig. 9 shows the power spectrum from the AE data processed in the same manner with the spectral amplitudes also in dB (counts^2 Hz^{-1}). For both data sets, the 95% confidence limits are 12.1 dB and -5.1 dB.

Dominant spectral peaks significant at the 4σ level are apparent in the strain spectrum at approximately 24 hours and 12 hours. Because of the short record length these peaks are not split at the various tidal periods (O_1, k_1, S_1, M_1, etc., at approximately 24 hours and O_2, k_2, S_2, M_2 etc., at approximately 12 hours). The spectral peaks in these strain data were analyzed more carefully using a larger data set so the contributions at the various tidal periods could be clearly identified. A spectrum utilizing three years of data is shown in Fig. 10. At about 12 hours the primary power is derived from tidal strain at the M_2 period (12.42 hours) while at about 24 hours the primary power is derived from either tidal strain at the S_1 period (24 hours) and perhaps some thermoelastic strains at the same period. Peak power in both frequency bands is comparable. The situation is less clear for the spectrum from the AE data. Spectral peaks do occur at approximately 24 and 12 hours respectively but these are significant only at the 2σ level. Because of the limited data and difficulty in obtaining more data, we cannot analyze these spectral peaks in more detail at this point.

We have examined correlation between the strain and AE data using the methods of cross-spectral analyses (Bendat and Piersol, 1966). These methods should reveal coherence between the two time series as a function of frequency. Let x(t) and y(t) represent the two time series and $X(\omega)$ and $Y(\omega)$ their Fourier transforms; the elements of the cross-spectral matrix are given by

$$|X(\omega)|^2 \mathrm{Re}\langle X^*(\omega)Y(\omega)\rangle = |C_{11}(\omega)C_{12}(\omega)|$$

$$\mathrm{Im}\langle X^*(\omega)Y(\omega)\rangle |Y(\omega)|^2 = |C_{21}(\omega)C_{22}(\omega)|.$$

To obtain smoothed spectral estimates, the data series are divided into D sections and a cross-spectral matrix is calculated for each section. The average cross-spectral matrix with 2D degrees of freedom is then determined. The squared coherence R^2

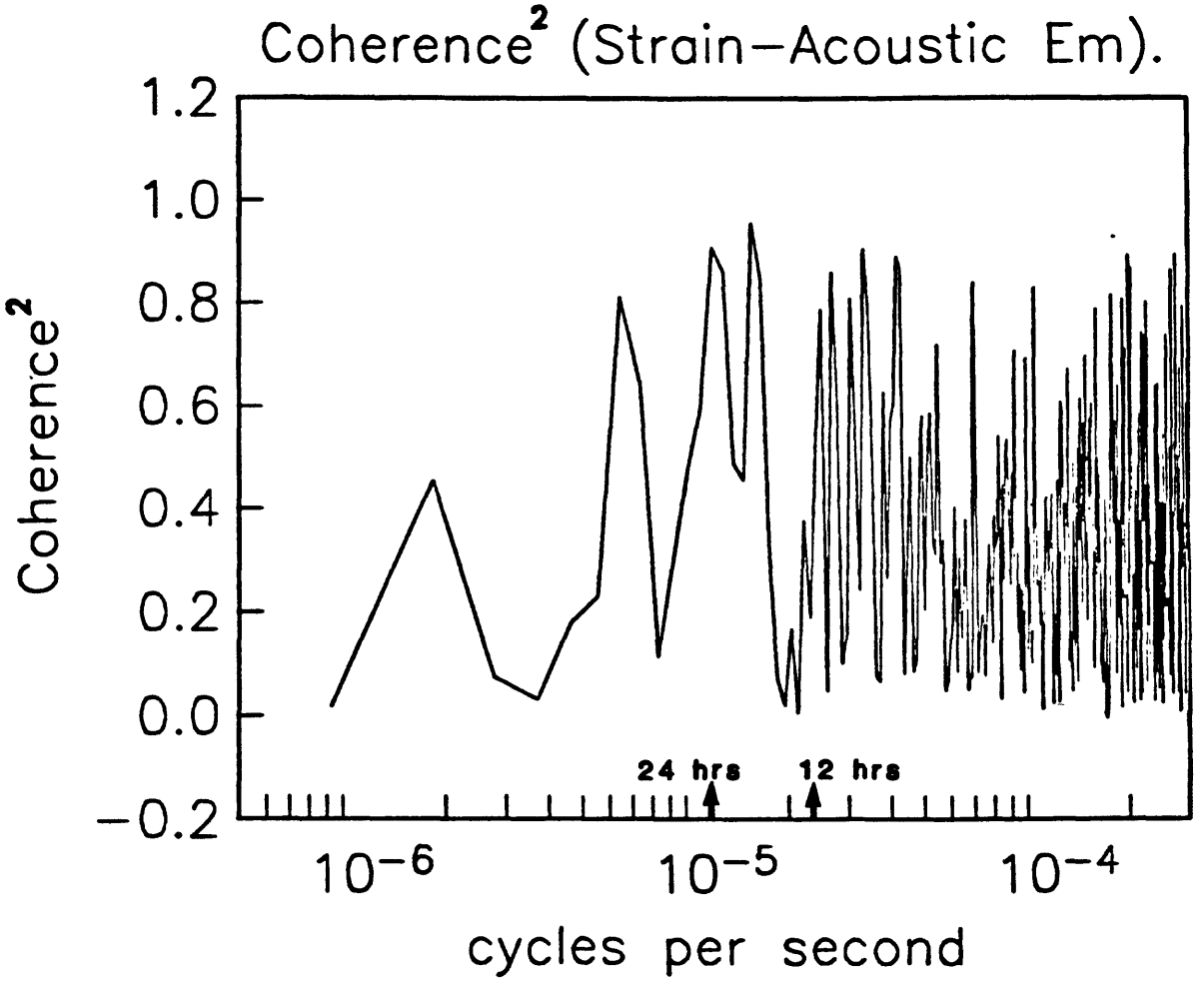

Fig. 11. The square of the coherence between the strain and acoustic emission data for 20 degrees of freedom as a function of frequency.

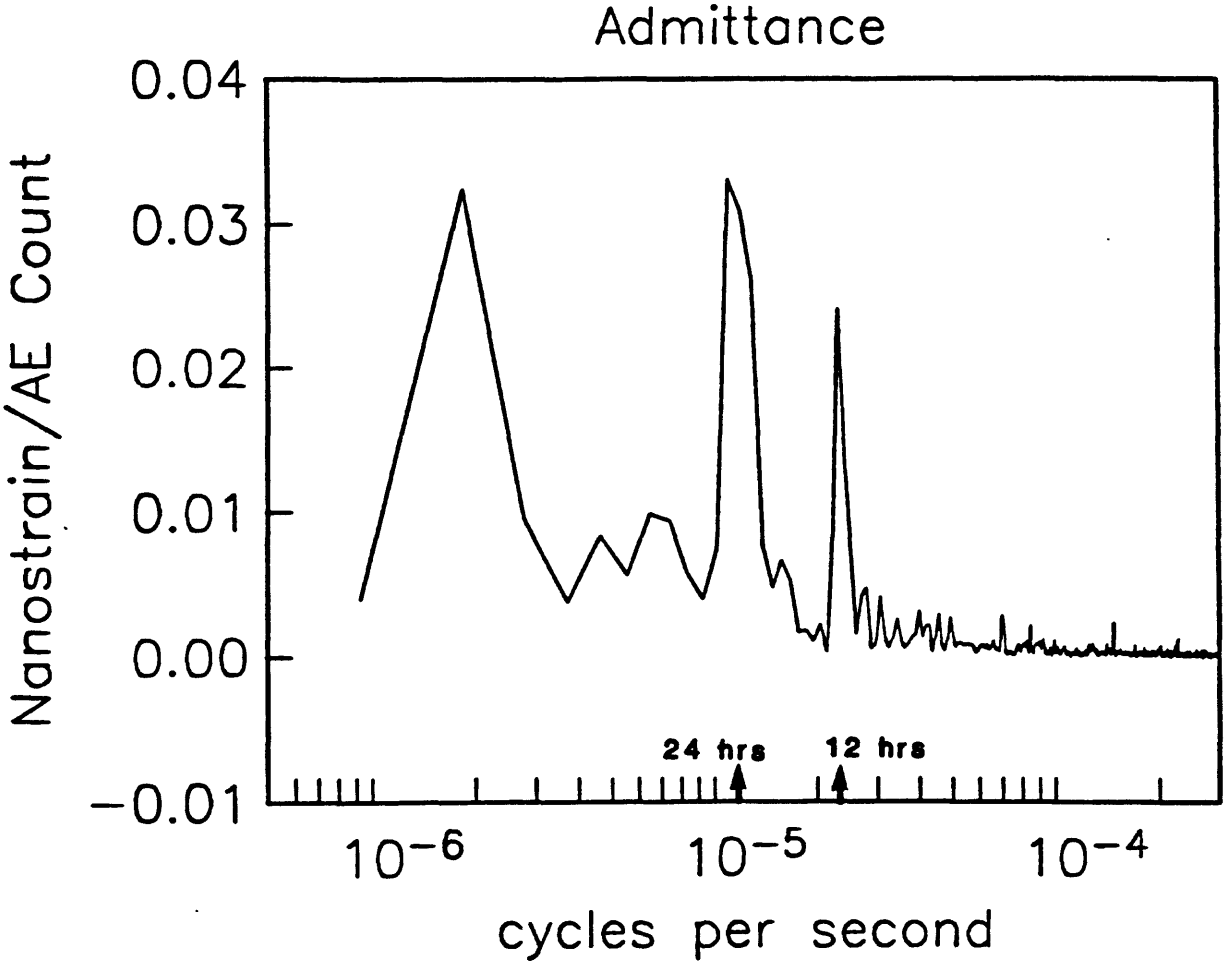

Fig. 12. Plot of admittance in nanostrain/count between the strain and acoustic emission data sets.

between the two series is estimated using

$$R^2 = \frac{\overline{(C_{12}^2 + C_{21}^2)}}{\overline{C_{11} C_{22}}}$$

where the bar represents averaging the results from the D time segments. Limits on the accuracy of this estimate are pointed out by Haubrich (1965). The squared coherence between the strain and AE data for 20 degrees of freedom is shown in Fig. 11. After correction for the finite length of the data set the only significant coherence between strain and AE data occurs at a period of 24 hours. While phase and admittance can also be calculated between the two data sets, we note, however, that these will not have much meaning unless significant coherence exists in a particular frequency band. Fig. 12 shows a plot of admittance in units of nanostrain/count between the two data sets. The value of admittance between strain and acoustic emission at diurnal periods is 0.03 nanostrain/count.

Two possibilities exist. Either tidal strains or perhaps some thermoelastic strains at diurnal periods are triggering AE. In either case, the strains are 10^{-7} or less. The important issue is not so much the particular source of the strain, but rather that diurnal and semi-diurnal strain changes of about 100 nanostrain are modulating the AE rate at a few counts/10 minute interval. This suggests that AE production occurs at strain rates even lower than those estimated to be caused by passage of seismic waves from various earthquakes. We believe these to be the lowest strain levels and strain rates for which acoustic emission has been observed.

6. CONCLUSION

Our observations at the Presidio in San Francisco demonstrate existence of AE associated with passage of seismic waves from earthquakes with magnitudes in the range of 4 to 5 and epicenters at distances from about 25 to 85 km away. The seismic waves from these earthquakes are estimated to have strain amplitudes of $\approx 10^{-7}$ and lower. Abrupt AE increases ranging from 35 to 470 events on three different AE sensors were clearly identifiable above the background at the times of the August 8 and November 4, 1989 Lake Elsman and Hayward fault earthquakes, respectively. It is also interesting that a much higher than normal background rate of AE was observed during the aftershock period following the Loma Prieta earthquake of October, 1989.

The background AE is weakly correlated with the tidal/thermoelelastic strains in the bunker, and we infer that the former is primarily responsible because the tidal strains dominate the thermoelastic strains at semi-diurnal periods (Fig. 10). The production of AE at such low strain-increment levels and rates independently supports the finding of AE at the higher strain levels and rates associated with passage of seismic waves from the Lake Elsman and Hayward fault earthquakes of 1989. We believe that these strain levels and strain rates are the lowest for which AE has been produced and reported in the literature.

7. ACKNOWLEDGEMENTS

We thank Alan Jones for his patient and long-term assistance to us in facilitating our access and interpretation of the data from the USGS instruments in the Presidio Observatory. We are indebted to Allen Green for his enthusiastic support and loan of

equipment for this work, and to Willie Lee for encouragement. We appreciate the insightful suggestion by Alan Lindh and Bill Bakun that we "field test" our ideas and equipment at the Presidio Observatory before attempting more ambitious undertakings elsewhere. Finally, we thank Dave Lockner for his comments on the draft manuscript.

8. REFERENCES

Armstrong, B.H., 1983. Acoustic Emission from Foreshocks and Secular Strain Changes Prior to Earthquakes, *EOS* **64**, 259.

Armstrong, B.H., and Stierman, D.J., 1989. Acoustic Emission from Foreshocks and Secular Strain Changes prior to Earthquakes, in *Acoustic Emission/ Microseismic Activity in Geologic Structures and Materials*, Proceedings of the Fourth Conference, Trans Tech Publications Clausthal-Zellerfeld, F. R. Germany, 309-326.

Armstrong, B.H., and Valdes, C.M., 1991. Acoustic Emission/Microseismic Activity at Very Low Strain Levels, in *Acoustic Emission: Current Practice and Future Directions*, ASTM STP 1077, W. Sachse, J. Roget, and K. Yamaguchi, Eds., American Society for Testing and Materials, Philadelphia, 358-364.

Bendat, J.G., and Piersol, A.G., 1966. *Measurement and Analysis of Random Data*, John Wiley and Sons, N. Y., 355 pp.

Borcherdt, R.D., Johnston, M.J.S., and Glassmoyer, G., 1989. On the Use of Volumetric Strain Meters to Infer Additional Characteristics of Short-Period Seismic Radiation, *Bull. Seism. Soc. Am.* **79**, 1006-1023.

Diakonov, B.P., Karryev, B.S., Khavroshkin, O.B., Nikolaev, A. V., Rykunov, L.N., Seroglasov, R.R., Trojanov, A.K., and Tsyplakov, V.V., 1990. Manifestation of earth deformation processes by high-frequency seismic noise characteristics, *Phys. Earth Planet. Inter.* **63**, 151-162.

Galperin, E.I., Petersen, N.V., Sitnikov, A.V., and Vinnik, L.P., 1990. On the properties of short-period seismic noise, *Phys. Earth Planet. Inter.* **63**, 163-171.

Hardy, H.R., Jr., and Ersavci, M.N., 1988. High Frequency Acoustic Emission/Microseismic Studies Associated with Structural Instability in Underground Mines, *Proceedings Second International Symposium on Rock Bursts and Seismicity in Mines*, Minneapolis, June 1988, Reprint Volume, University of Minneapolis, 279-294.

Hardy, H. R., Jr., Belesky, R.M., and Mrugala, M., 1988. AE/MS Activity in Rock at very Low Stresses, paper presented at the 9th International Acoustic Emission Symposium, Japanese Society for Non-Destructive Inspection, Kobe, Japan, Nov. 14-17.

Haubrich, R.A., 1965. Earth Noise, 5-500 millicycles per second, 1, Spectral Stationarity, Normality, and Nonlinearity, *Jour. Geophys. Res.* **70**, 1415 -1427.

Jones, A.C., 1983. Description and History of Mercury-Tube Tiltmeters Used in the San Francisco Bay Area, California, Open-File Report 83-463, U. S. Geological Survey, Menlo Park, CA, June, 1983.

Lockner, D., Byerlee, J.D., Kuksenko, V., Ponomarev, P., and Sidorin, A., 1991. Quasi-static fault growth and shear fracture energy in granite, *Nature* **350**, 39-42.

Lord, A.E., Jr., 1975. Acoustic Emission, in *Physical Acoustics, Principles and Methods, Vol. XI*, Ed. by W. P. Mason and R. N. Thurston, Academic Press, N. Y., 290-353.

Lord, A.E., Jr., 1981. Acoustic Emission - - an Update, in *Physical Acoustics, Principles and Methods, Vol. XV*, Ed. by W. P. Mason and R. N. Thurston, Academic

Press, N. Y., 295-360.

Lord, A.E., Jr., 1982. On the Sensitivity of the Acoustic Barkhausen/Magnetomechanical Acoustic Emission Effect, *J. Acoustic Emission* **1**, 193-194.

Momoh, O., Bawden, W.F., and Kandut, H.H., 1989. AE/MS Monitoring in Noranda Group Mines, in *Acoustic Emission/ Microseismic Activity in Geologic Structures and Materials*, Proceedings of the Fourth Conference, ed. by H. R. Hardy, Jr., Trans Tech Publications, Clausthal-Zellerfeld, F. R. Germany, 189-206.

Repsher, R.C. and Steblay, B.J., 1985. Structural Stability Monitoring Using High-Frequency Microseismics, *Proceedings 26th U. S. Symposium on Rock Mechanics*, (Rapid City, SD, June, 1985), Vol. 2, A. A. Balkema, Rotterdam/Boston, 707-713.

Richter, C.F., 1958. *Elementary Seismology*, W. H. Freeman and Co., Inc., San Francisco, 768 pp.

Valdes, C.M. and Armstrong, B.H., 1989. Kilohertz Acoustic Emission Monitoring at the Presidio, San Francisco, During the M_L = 5.1 Lake Elsman Earthquake of August 8, 1989, *EOS* **70**, 1224.

Vladut, T.L., and Lepper, C.M., 1989. Early Warning of Slope Instabilities by Microseismic Monitoring, in *Acoustic Emission/ Microseismic Activity in Geologic Structures and Materials*, Proceedings of the Fourth Conference, ed. by H. R. Hardy, Jr., Trans Tech Publications, Clausthal-Zellerfeld, F. R. Germany, 511-530.